Low-kinetic energy impact response of auxetic and conventional open-cell polyurethane foams

ALLEN, Tom, SHEPHERD, Jonathon, HEWAGE, Trishan M, SENIOR, Terry <http://orcid.org/0000-0002-3049-5724>, FOSTER, Leon <http://orcid.org/0000-0002-1551-0316> and ALDERSON, Andrew <http://orcid.org/0000-0002-6281-2624>

Published version

ALLEN, Tom, SHEPHERD, Jonathon, HEWAGE, Trishan M, SENIOR, Terry, FOSTER, Leon and ALDERSON, Andrew (2015). Low-kinetic energy impact response of auxetic and conventional open-cell polyurethane foams. physica status solidi b, 252 (7), 1631-1639.

Low-kinetic energy impact response of auxetic and conventional open-cell polyurethane foams

T. Allen[2], J. Shepherd,[1,2] T.M. Hewage,[3] T. Senior[2], L. Foster,[2] & A. Alderson[3]

[1]Griffith University, Gold Coast Campus, Parklands Drive, Southport, 4215, Australia

[2]Centre for Sports Engineering Research, Sheffield Hallam University, Howard Street, Sheffield S1 1WB, UK

[3]Materials and Engineering Research Institute, Sheffield Hallam University, Howard Street, Sheffield S1 1WB, UK

Abstract - This paper reports quasi-static and low-kinetic energy impact testing of auxetic and conventional open-cell polyurethane foams. The auxetic foams were fabricated using the established thermo-mechanical process originally developed by Lakes. Converted foams were subject to compression along each dimension to 85% and 70% of the unconverted dimension during the conversion process, corresponding to linear compression ratios of 0.85 and 0.7, respectively. The 0.7 linear compression ratio foams were confirmed to have a re-entrant foam cell structure and to be auxetic. Impact tests were performed for kinetic energies up to 4 J using an instrumented drop rig and high speed video. A flat dropper was employed on isolated foams, and a hemisperical shaped dropper on foams covered with a rigid polypropylene outer shell layer. The flat dropper tests provide data on the rate-dependency of the Poisson's ratio in these foam test specimens. The foam Poisson's ratios were found to be unaffected by the strain rate for the impact energies considered here. Acceleration-time data are reported along with deformation images from the video footage. The auxetic samples displayed a 6 times reduction in peak acceleration, showing potential in impact protector devices such as shin or thigh protectors in sports equipment applications.

1. Introduction

Protective sporting equipment can prevent acute injuries (Hergenroeder, 1998; Adirim and Cheng, 2003) and be cost effective when compared to direct medical costs (Bahr, 2005). For the equipment to be effective, injury mechanisms, load ranges, human tolerances and material performance all need to be understood

(McIntosh, 2012). Protective equipment usually performs impact energy attenuation, acceleration management, load distribution and force limitation. Foams often serve as the energy absorbing component, while a shell can be utilised to enable more foam to be compressed for a given impact (Ankrah and Mills 2003; Ankrah and Mills, 2004, Mills, 2003). Often the materials used are effective in general use but not for the range of impacts which can occur throughout the sport.

Sanami et al. (2014) present a case for applying auxetic foams to protective sporting equipment. Auxetic materials have a negative Poisson's ratio, when placed under compression in one direction they become thinner in one or more perpendicular directions (Evans et al. 1991). The general mechanism of obtaining auxetic foam from conventional foam consists of three steps: (i) compression of foam, (ii) softening it to release stress at the compressed state, and (ii) stiffening the densified but already unstressed foam. The traditional approach is to use a thermo-mechanical process (Lakes, 1987), although a chemo-mechanical process can also be applied (Grima, Attard, Gatt, et al., 2009). Auxetic foams have some interesting mechanical properties including, synclastic curvature and improved resilience (Lakes 1987), indentation resistance (Lakes and Elms 1993; Chan and Evans 1998), shear resistance (Choi and Lakes 1992), fracture toughness (Choi and Lakes 1992), energy dissipation (Lakes and Elms 1993, Bezazi and Scarpa 2007), vibration damping (Howell et al. 1991, Chen and Lakes 1996). In certain density regions auxetic foams and isotropic auxetic continua can also display negative Bulk Modulus (Moore, et al., 2006; Lakes, 2008) and negative compliance (Grima, Caruana-Gauci, Wojciechowski, et al., 2013; Pozniak, Kaminski, Kedziora, et al., 2010).

Impact and indentation investigations have previously been reported on auxetic polymeric (Ge 2013, Lisiecki et al 2013a and 2013b, Lim et al 2014, Lakes and Lowe 2000, Scarpa et al 2002) and metallic (Lakes and Elms 1993) foams, sandwich panels comprising kevlar fabric-epoxy honeycomb core and fibre-reinforced polymer skins (Hou et al 2014), carbon fibre-reinforced epoxy laminates (Alderson and Coenen 2008), polymers containing auxetic chopped fibres (Uzun 2012), and microporous polymers (Alderson et al 2000). A number of theoretical treatments are also present in the literature (Argatov et al 2012, Lakes 1993, Kocer et al 2009, Wang and Lakes 2002, Schultz et al 2011, and Qi et al 2013).

Under impact loading, auxetic materials have been shown to offer increased energy absorption (Ge 2013, Lisiecki et al 2013a, Lim et al 2014, Lakes and Elms 1993, Uzun 2012, and Hou et al 2014), higher impact resistance (Hou et al 2014, Alderson and Coenen 2008, Uzun 2012, Alderson et al 2000, Kocer et al 2009 and Lakes 1993) and reduced damage area (Hou et al 2014, Alderson and Coenen 2008 and Uzun 2012). The impact resistance appears to be rate dependent in carbon-epoxy laminates (Alderson and Coenen 2008), and auxetics appear to be more prone to surface failure under quasi-static and low velocity impact (Lim et al 2014, Argatov et al 2012) although this is mitigated when a surface layer is placed over the auxetic material (Argatov et al 2012).

Auxetics have been reported to display higher maximum deceleration during impact (Lisiecki et al 2013a), which would be expected to lead to increased pressure and, therefore, be detrimental for cushioning applications. However, this is contrary to measurement of lower maximum seating pressure (Lakes and Lowe 2000) and an analytical approach (Wang and Lakes 2002) which shows negative Poisson's ratio cushions reduce the peak pressure if the cushion shear modulus is held constant as Poisson's ratio is varied. In the case of the cushion Young's modulus being held constant, Wang and Lakes show the optimal Poisson's ratio is zero. Auxetic materials have been suggested to offer the best solution for reducing impact forces which may be distributed over a wide area (e.g. person's back) or a narrow area (e.g. elbow) in, for example, wrestling mat or knee pad applications (Lakes, 1993).

Sanami et al (2014) applied the thermo-mechanical process to open-cell polyurethane foam, reporting a reduction in Poisson's ratio from 0.36 to -0.22. Their conventional foams exhibited classical behaviour under quasi-static compression, the stress-strain curve was linear until ~5% strain and then entered a plateau region (Gibson & Ashby 1988). In agreement with Lakes (1987) the auxetic foam showed higher resilience, Young's modulus was initially only 15 kPa in comparison to 35 kPa for the conventional foam, but the stress-strain curve showed an extended region of linear elasticity up to maximum compression at 15% strain. Their auxetic foams also absorbed more than double the energy than their conventional counterparts under

quasi-static indentation with a sphere. Increased resilience (Scarpa et al 2002, Pastorino 2007) has also been observed in auxetic open-cell polyurethane foams at high compressive strain rates. The effect of strain rate on the strain-dependent negative Poisson's ratios in auxetic foams has also been investigated (Pastorino 2007). Several different foam types were considered and no universal trend with strain rate was observed in response to strain rates up to 9 s^{-1}.

Standards for protective sporting equipment usually include an impact test/s, with the pass criterion based on the ability to keep accelerations or transmitted forces below a specified level (e.g. BS 6183-1:1981). The literature on auxetic foams indicates they have potential to be applied to produce protective equipment with superior energy absorption and/or reduced thickness. Further work is required to determine the ability of auxetic foams to attenuate impact forces and/or accelerations, to investigate the rate-dependency of the auxetic property on impact response, and to establish the effect of a semi-rigid surface layer on the impact response of the auxetic foam. The aim of this paper is to investigate these issues by determining the impact performance of auxetic open-cell polyurethane foam. The findings will be discussed in relation to the application of auxetic foam to protective sporting equipment.

2. Methods

This research focussed on quasi-static and low-kinetic energy impact testing to characterise auxetic foams - fabricated with the thermo-mechanical conversion process - in comparison to their conventional counterparts. Through thickness images of the cell structure of the foams were also obtained using a camera (Canon EOS 5D Mark II with EF100mm f/2.8L Macro IS USM lens) on manual exposure. Impact testing was performed with foams in isolation and foams covered with a polypropylene sheet to replicate protective sporting equipment. Performance was based on the ability of the foams to attenuate impact acceleration.

Table 1 shows the materials used, the foams were reticulated open-cell polyurethane, designated by R30FR with 30 pores in^{-1}, R45FR with 45 pores in^{-1} and R60FR with 60 pores in^{-1} (Custom Foams). R45FR corresponds to the foam utilised

by Sanami et al. (2014) and the unconverted foams had similar densities to those investigated by other authors (Scarpa et al 2002, Pastorino et al 2007). Association football shin guards often utilise ethylene vinyl acetate copolymer foams with densities of around 70 to 100 kgm^{-3} (Ankrah and Mills, 2003), and the conversion process used here resulted in foams with densities within this range. The foam samples tested had dimensions of 75 x 75 x 20 mm and the polypropylene sheets (Direct Plastics, PPH / PP-DWST - Homopolymer) had dimensions of 75 x 75 x 1 mm. The thickness of the foam samples was representative of typical protective sporting equipment. The unconverted foam test samples were cut to size from a monolith.

To facilitate the thermo-mechanical conversion process samples exceeding the test dimensions were cut from a monolith. These samples were 118 x 118 x 118 mm for a Linear Compression Ratio (LCR) of 0.85 and 143 x 143 x 143 mm for a LCR of 0.7. Linear compression ratio is defined as the ratio of the compressed to initial dimensions. The foams were placed inside a compression mould of size 100 x 100 x 100 mm to achieve a triaxial compression, with lubricant applied to reduce edge creasing. The mould containing the compressed foam was placed in an oven at 200°C. After 30 minutes the mould was removed from the oven, and the foam was taken from the mould and stretched gently by hand in each of the three directions at room temperature to avoid adhesion of the cell ribs. The foam was reinserted into the mould and placed back into the oven at 200°C for a further 30 minutes. The process was repeated for a final time with the oven temperature reduced to 100°C for 30 minutes.

Quasi-static compression tests were performed on three samples of each material in a uniaxial test machine (Instron 3369, fitted with a 50 kN load cell). The samples were compressed to 50% strain at a rate of 10 mm/min, with load and extension recorded at 10 Hz. Young's moduli were obtained from linear regression up to 5% compressive strain, which is within the region of linear elasticity (Gibson & Ashby, 1988; Sanami et al. 2014).

Low-kinetic energy impact tests were performed using a bespoke drop rig (Figure 1). A cylindrical flat faced dropper (2.27 kg and 115 mm diameter face) was employed

on foams in isolation and a hemispherical faced dropper (2.09 kg and 73 mm diameter hemisphere) was employed when the foams were covered with the polypropylene sheet. The flat dropper applied a distributed load to the entire face of the sample, while the hemispherical dropper applied a concentrated load at the centre of each composite (foam plus sheet) sample. The sheet was sufficiently thin to provide intermediate behaviour between a concentrated load and an evenly distributed load, as shown in Figure 2. Drop heights were set at 0.1 and 0.2 m for the flat dropper and 0.1 m for the hemispherical dropper, providing impact energies of ~2 and ~4 J. The dropper was fitted with a wireless accelerometer (PCB, ICP Shock Sensor, 350B24) recording at 50,000 Hz, providing acceleration-time data for each impact (DTS SLICEWare Version 1.08.0475). Five samples of each material were tested in each of the 3 scenarios, requiring 15 samples of each material.

Poisson's ratios were obtained from the quasi-static tests and flat faced dropper impact tests. Measurements of Poisson’s ratio were not obtained for the hemispherical dropper tests because the load was not evenly distributed. The quasi-static tests were filmed with a network camera (Axis P1357) at 25 Hz, with a resolution of 1080 x 720 pixels and the impact tests were filmed with a high-speed camera (Vision Research, Phantom V4.3) at 10,000 Hz, with a resolution of 416 x 128 pixels and exposure time of 97 μs. The video footage was used to locate temporal centre positions of four marks applied to the front face of each sample, using a bespoke tracking software utilising MATLAB (MathWorks). True strains were calculated in both directions and Poisson's ratios were obtained from linear regression, in the region up to 10% compression. Only tests with a Root Mean Squared Error between the linear model and data below 0.005 were used, resulting in inclusion levels of 96% for quasi-static compressions, 82% for 0.1 m impacts and 87% for 0.2 m impacts. Comparison with manual analysis verified the accuracy of the tracking algorithm.

Footage from the impact tests was also used to identify the frames corresponding to the start and end of contact between the sample and dropper, and the maximum deformation. Aligning peak acceleration with maximum deformation allowed the start and end of contact to be identified in the acceleration-time traces. Repeated analysis

of 10 randomly selected impacts indicated uncertainties in contact time to be within 1 ms.

3. Results

Figure 3 shows differences in the pore structures between the unconverted and converted foams. The unconverted foam and the converted foam with an LCR of 0.7 exhibit the regular open-cell and re-entrant structures, respectively, characteristic of positive Poisson's ratio and auxetic foams (Lakes 1987, McDonald et al 2011). The structure of the foam converted with an LCR of 0.85 is seen to be intermediate between the other two foams, consistent with the intermediate level of compression applied in this case.

Figure 4 shows the classical stress-strain relationship for the unconverted foam, with the start of the plateau region corresponding to cell-wall buckling occurring around 5-10% compression. The foams with the LCR of 0.7 exhibited approximately half the Young's modulus of the unconverted foam (Table 2), in agreement with Sanami et al (2014). These re-entrant structured foams showed no significant plateau region up to maximum compression at 50% strain, indicating higher resilience. The foam with the LCR of 0.85 showed intermediate behaviour, with reduced Young's modulus in the linear region up to approximately 15% strain followed by a plateau region at higher strain.

Figure 5 shows nonlinear lateral strain-longitudinal strain relations for the unconverted foam and foams with a LCR of 0.85, with the data following a similar trend to the corresponding quasi-static stress-strain plots. The foams with a LCR of 0.7 exhibited lower lateral strain for a given longitudinal strain and did not show a significant plateau region. Table 2 confirms that Poisson's ratio decreased with LCR, with similar values obtained for each LCR from the quasi-static and impact tests. The foams with the LCR of 0.7 showed marginally auxetic behaviour, as indicated by the re-entrant pore structure and near linear quasi-static stress-strain relationship.

Figure 6 shows sample acceleration-time traces for the flat dropper impacts. For each of the foams peak accelerations increased with impact energy. The

acceleration-time traces for the unconverted foams show a dramatic increase in acceleration corresponding to the point of maximum deformation. The traces for the auxetic foams with a LCR of 0.7 had lower and less pronounced peaks, with a more gradual change in acceleration throughout impact. The foam with a LCR of 0.85 showed intermediate behaviour.

Figure 7 confirms peak accelerations for the flat faced dropper decreased with LCR. Peak accelerations for the auxetic foams with the LCR of 0.7 were ~40% of those for the unconverted foams. Figure 8 shows contact times and times to maximum deformation for this dropper were lower when the impact energy was 4 J in comparison to 2 J. For each drop height, similar contact times were observed for the unconverted foam and foams with a LCR of 0.85. Contact times for the foams with a LCR of 0.7 where ~25% shorted than those observed for the other foams. For each drop height, times to maximum deformation were similar for all foams, indicating a shorter restitution phase for the foams with a LCR of 0.7. Assuming full deformation of the samples, the average loading rate for the impacts was in the region of 80,000 to 120,000 mm/m.

Figure 9 shows sample acceleration-time traces for the hemispherical dropper. The dramatic increase in acceleration at ~15 ms for the unconverted foam indicates the sample bottomed out, as confirmed in Figure 10a. In contrast, Figure 9c shows the auxetic sample with the LCR of 0.7 contracted laterally, densifying around the dropper and preventing bottoming out. The corresponding acceleration-time trace in Figure 9 shows a lower and less pronounced peak with a more gradual change in acceleration throughout impact. The foam with a LCR of 0.85 showed intermediate behaviour. Figure 11 confirms peak accelerations for the hemispherical dropper decreased significantly with LCR. Peak accelerations for the auxetic foams with the LCR of 0.7 were ~80% lower than those observed for the unconverted foam.

4. Discussion

Peak accelerations for a hemispherical dropper with 2 J of energy were ~6 times lower when impacting auxetic foams covered with a thin polypropylene sheet, in comparison to their conventional counterparts. The effect of the sheet-foam

thickness ratio and the mechanical properties of the sheet, on the impact performance of the composite pads, warrants further investigation. Figure 2 clearly shows sheet thickness can have a dramatic effect on load distribution for the underlying foam. This will be the focus of further research, along with the potential to tailor the mechanical properties of the shell. In this latter case, the ability to introduce the auxetic effect may be achieved in a carbon fibre-reinforced epoxy laminate shell (Alderson & Coenen, 2008), for example.

For foams in isolation impacted with a flat mass with energies up to 4 J, peak accelerations were ~3 times lower for auxetic foams in comparison to the conventional foams. The significant reduction in peak accelerations for the auxetic foams was because they prevented bottoming out. No clear differences were observed in peak accelerations between levels of foam porosity in the range 30 to 60 pores in^{-1}.

Through thickness images and quasi-static compression testing indicated differences between conventional foams and those subjected to a thermo-mechanical conversion process. The unconverted foams exhibited classical stress-strain behaviour, with cell-wall buckling occurring at around 5 to 10% compression (Gibson & Ashby, 1988; Sanami et al. 2014). Foams with a LCR of 0.7 had a re-entrant structure and stress-strain curve without a significant plateau region in agreement with Sanami et al. (2014), remaining close to linear up to maximum compression at 50% strain. The auxetic foams exhibited approximately half the Young's modulus of their conventional counterparts, and the modulus values matched those reported Sanami et al. (2014).

Quasi-static and low-kinetic energy impact testing resulted in comparable values for Poisson's ratio across each of the three levels of foam conversion. Poisson ratios for the unconverted foams fell slightly below the typical value of 0.3 for polyurethane (Gibson & Ashby, 1988) and were lower than the value of 0.36 reported by Sanami et al. (2014). Negative Poisson's ratios were reported for converted foams for average loading rates up to ~120,000 mm/m. However, Poisson's ratios for foams with a LCR of 0.7 fell only just below zero, considerably higher than values reported in the literature for similar foams following a thermo-mechanical conversion process

(Sanami et al., 2014; Friis et al., 1988; Chen et al., 1997; Wang et al., 2001; Bianchi et al., 2008). The Poisson's ratio of auxetic foam is likely to be a function of the conversion process – sample size and shape, LCR and conversion time and temperature – and the specific methodology for which it is measured, including the sample shape and strain range.

In this work Poisson's ratio has been determined on very low aspect ratio (short height and large lateral dimensions) test specimens to enable investigation of strain rate. In view of the successful production of the required foam structure for auxetic behaviour, the low aspect ratio specimen geometry may be the main factor for the reduction in magnitude of Poisson's ratio compared to previous reports. Friction effects associated with the surface on which the foams are placed, and the surface of the compression plate/flat dropper, will restrict lateral movement of the foam in contact with these surfaces. For low aspect ratio specimens, edge effects due to frictional constraints at the top and bottom foam surfaces will dominate the overall lateral response of the foam. Compression testing of auxetic foam samples with different aspect ratios could help further our understanding of edge effects on the Poisson's ratio response and, therefore, the utility of auxetic foams in applications where foam thickness constraints in the design phase are significant. Further work will, nevertheless, be undertaken to optimise the conversion process with the aim of minimising Poisson's ratio.

The foundational work presented here has shown further potential for auxetic foams to be applied to protective sporting equipment. Future work will also include investigations into other base foams, focussing on their ability to be converted to auxetic foams and impact performance following conversion. Testing of these foams will also be undertaken across a wider range of impact energies and for repeated impact loading. Auxetic foam samples larger than those tested here will also need to be produced, so prototype protective sporting equipment utilising these foams can be developed and assessed against the appropriate standard.

5. Conclusion

Auxetic foams have shown potential to be applied to protective sporting equipment. These foams reduced impact peak accelerations by ~6 times in comparison to their conventional counterparts, when impacted with a rigid hemisphere the size of a cricket ball. Negative Poisson's ratios were observed for average loading rates up to ~120,000 mm/m, although the values for Poisson's ratio were not as low as those reported in the literature. Further work will aim to optimise both foam selection and the conversion process. Applying auxetic foams to protective sporting equipment while assessing performance against the appropriate testing standard is now required.

6. Acknowledgements

We are grateful to funding from Sheffield Hallam University via the IMAGINE project for this work. The authors would like to thank Nicolo Martinello for his assistance.

7. References

Adirim T. A. and Cheng T. L. (2003) Overview of Injuries in the Young Athlete, Sports Med, 33:1, pp 75-81

Ankrah S. and Mills N.J. (2003) Performance of football shin guards for direct stud impacts, Sports Engineering, 6:4, pp 207-219.

Ankrah S. and Mills N. J. (2004) Analysis of ankle protection in Association football

Sports Engineering, 7:1, pp 41-52.

Alderson K. L. and Coenen V. L. The low velocity impact response of auxetic carbon fibre laminates. phys. stat. sol. (b) 245, No. 3, 489–496 (2008)

Alderson, K. L., Fitzgerald, A., & Evans, K. E. (2000). The strain dependent indentation resilience of auxetic microporous polyethylene. Journal of Materials Science, 35, 4039–4047.

Argatov I. I., Guinovart-Díaz R, Sabina F. J. On local indentation and impact compliance of isotropic auxetic materials from the continuum mechanics viewpoint. International Journal of Engineering Science 54 (2012) 42–57.

Bahr, R., & Krosshaug, T. (2005). Understanding injury mechanisms: a key component of preventing injuries in sport. British Journal Of Sports Medicine, 39(6), 324--329.

Bezazi A and Scarpa F. Mechanical behaviour of conventional and negative Poisson's ratio thermoplastic polyurethane foams under compressive cyclic loading. Int J Fatigue 2007; 29: 922–930.

Chan, N., & Evans, K. (1997). Fabrication methods for auxetic foams. Journal Of Materials Science, 32(22), 5945--5953.

Chen, C.P., Lakes, R.S., 1996. Micromechanical Analysis of Dynamic Behavior of Conventional and Negative Poisson's Ratio Foams. Journal Engineering Materials and Technology 118, 285 - 288.

Choi, J.B., Lakes, R.S., 1992. Nonlinear Properties of Polymer Cellular Materials with a Negative Poisson's Ratio. Journal of Materials Science 27, 5375 - 4684.

Evans, K.E., Nkansah, M., Hutchison, I.J., Rogers, S.C., 1991. Molecular Network Design. Nature 353, 124.

Ge C. A comparative study between felted and triaxial compressed polymer foams on cushion performance. Journal of Cellular Plastics 2013 49: 521-533.

Gibson L. L., & Ashby M. F. (1988). Cellular solids. Structure & properties. Pergamon Press, Oxford. IX + 357 p. ISBN 0-08-036607-4

Grima J. N., Attard D., Gatt R., et al. Advanced Engineering Materials Volume: 11 Issue: 7 Pages: 533-535 Published: JUL 2009

Grima J. N., Caruana-Gauci R., Wojciechowski K. W., et al. Smart materials and structures Volume: 22 Issue: 8 Article Number: 084015 Published: AUG 2013

Hergenroeder, A. C. (1998). Prevention of sports injuries. Pediatrics, 101(6), 1057-1063. doi:10.1542/peds.101.6.1057

Hou Y., Neville R., Scarpa F., Remillat C., Gua B., Ruzzene, M. Graded conventional-auxetic Kirigami sandwich structures: Flatwise compression and edgewise loading. Composites: Part B 59 (2014) 33–42.

Howell, B., Prendergast, P., Hansen, L., 1991. Acoustic Behaviour of Negative Poisson's Ratio Materials, DTRC – SME - 91/01, David Taylor Research Centre, Annapolis, MD.

Kocer, C., McKenzie, D. R., & Bilek, M. M. (2009). Elastic properties of a material composed of alternating layers of negative and positive Poisson's ratio. Materials Science and Engineering A, 505 111–115.

Lakes, R. (1987). Foam Structures with a Negative Poisson's Ratio. Science, 235 (Febuary), 1038--1040.

Lakes R., Wojciechowski K. W., Physica Status Solidi B - Basic Solid State Physics Volume: 245 Issue: 3 Pages: 545-551 Published: MAR 2008.

Lakes, R. S. (1993). Design considerations for materials with negative Poisson's ratios. Transactions of the ASME – Journal of Mechanical Design, 115, 696–700.

Lakes, R. S., & Elms, K. (1993). Indentability of conventional and negative Poisson's ratio foams. Journal of Composite Materials, 27(12), 1193-1202. doi:10.1177/002199839302701203

Lakes, R. S. and Lowe, A. "Negative Poisson's ratio foam as seat cushion material", Cellular Polymers, 19, 157-167, July (2000).

Lim T. C., Alderson A., and Alderson K. L.. Experimental studies on the impact properties of auxetic materials. Phys. Status Solidi B 251, No. 2, 307–313 (2014)

Lisiecki J., Błazejewicz T., Kłysz S., Gmurczyk G., Reymer P., and Mikułowski G.. Tests of polyurethane foams with negative Poisson's ratio. Phys. Status Solidi B 250, No. 10, 1988–1995 (2013a)

Lisiecki J., Kłysz S., Błazejewicz T., Gmurczyk G., Reymer P. Tomographic examination of auxetic polyurethane foam structures. Phys. Status Solidi B, 1–7 (2013b)

McDonald S. A., Dedreuil-Monet G., Yao Y. T., Alderson A., and Withers P. J. In situ 3D X-ray microtomography study comparing auxetic and non-auxetic polymeric foams under tension. Phys. Status Solidi B 248, No. 1, 45–51 (2011)

McIntosh, A. (2012). Biomechanical considerations in the design of equipment to prevent sports injury. Proceedings Of The Institution Of Mechanical Engineers, Part P: Journal Of Sports Engineering And Technology, 226(3-4), 193--199.

Moore B., Jaglinski T., Stone D. S. et al., PHILOSOPHICAL MAGAZINE LETTERS Volume: 86 Issue: 10 Pages: 651-659 Published: OCT 2006

Mills NJ. Foams in sport, In: Jenkins MJ editor. Sport Materials, Woodhead, Cambridge, 2003, chapter 2.

Pastorino P, Scarpa F, Patsias S, Yates JR, Haake SJ, Ruzzene M, 2007. Strain rate dependence of stiffness and Poisson's ratio of auxetic open cell PU foams. Physica Status Solidi (b) 244 (3), 955-965.

Pozniak A. A. Kaminski H. Kedziora P. et al., Reviews on advanced materials science, Volume: 23 Issue: 2 Pages: 169-174 Published: MAY 2010

Qi C, Yang S, Wang D, and Yang L-J. Ballistic Resistance of Honeycomb Sandwich Panels under In-Plane High-Velocity Impact. The Scientific World Journal. Volume 2013, Article ID 892781, 20 pages

Sanami, M., Ravirala, N., Alderson, K., Alderson, A. (2014) Auxetic materials for sports applications, Proceedings of the 10th Conference on the Engineering of Sport, Procedia Engineering 72 (2014) 453 – 458.

Scarpa F, Yates JR, Ciffo LG, Patsias S, 2002. Dynamic crushing of auxetic open-cell polyurethane foam. Proceedings of the Institution of Mechanical Engineers, Part C: Journal of Mechanical Engineering Science 216(12), 1153-1156

Schultz, J. et al. Optimization of honeycomb cellular meso-structures for high speed impact energy absorption. Proceedings of the ASME 2011 International Design Engineering Technical Conferences. IDETC/CIE 2011 August 28-31, 2011, Washington, DC, USA. DETC2011-48000

Uzun, M. Mechanical Properties of Auxetic and Conventional Polypropylene Random Short Fibre Reinforced Composites. FIBRES & TEXTILES in Eastern Europe 2012; 20, 5(94): 70-74.

Wang, Y.-C., & Lakes, R. (2002). Analytical parametric analysis of the contact problem of human buttocks and negative Poissons ratio foam cushions. International Journal of Solids and Structures, 39, 4825–4838.

TABLES

Table 1 Materials used in this research.

Sample type	Density (kg/m^3)	Number
Conventional foam: R30FR, R45FR & R60FR	26-32	15 of each
Converted foam with LCR of 0.85: R30FR, R45FR & R60FR	42-52	15 of each
Converted foam with LCR of 0.7: R30FR, R45FR & R60FR	76-94	15 of each
Polypropylene sheet	905	15

Table 2 Material properties from quasi-static and dynamic characterisation averaged across all three foam types. Values for Young's modulus and Poisson's ratio correspond to region up to 5% and 10% compression, respectively.

			Poisson's ratio	
	Young's modulus (kPa)	Quasi-static	0.1 m	0.2 m
UC	35 ± 1	0.29 ± 0.20	0.24 ± 0.13	0.26 ± 0.11
0.85LCR	20 ± 10	0.05 ± 0.12	0.04 ± 0.07	0.09 ± 0.13
0.7LCR	18 ± 6	-0.01 ± 0.03	-0.01 ± 0.06	-0.04 ± 0.05

FIGURES

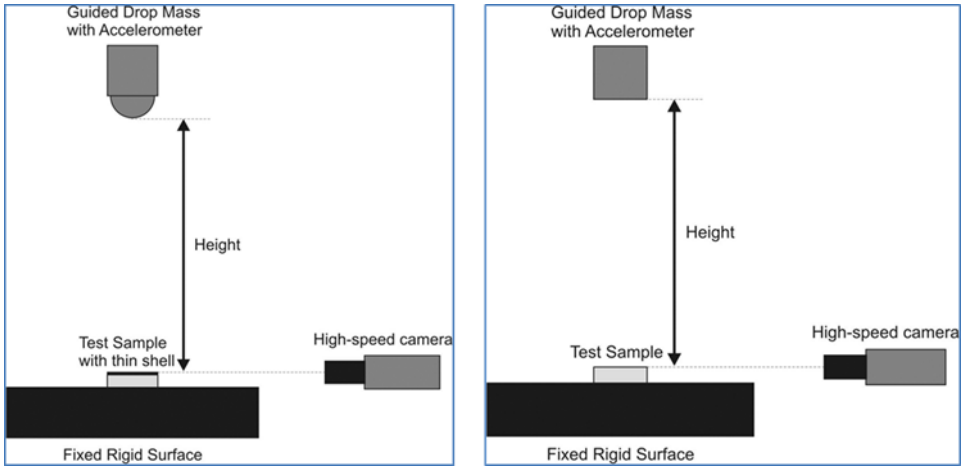

Figure 1 Experimental setup for impact testing consisting of a bespoke instrumented drop rig and high speed camera, a) hemispherical dropper and b) flat dropper. The diameter of the hemispherical dropper corresponded to the value specified in the standard for protective equipment for cricketers (BS 6183-1:1981).

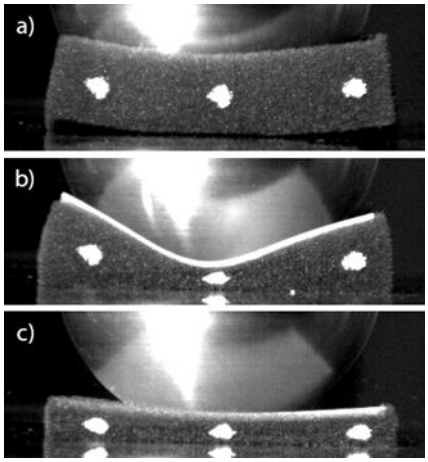

Figure 2 Maximum deformation of the hemispherical dropper on conventional R60 foam with a) no sheet, b) 1 mm sheet and c) 2 mm sheet.

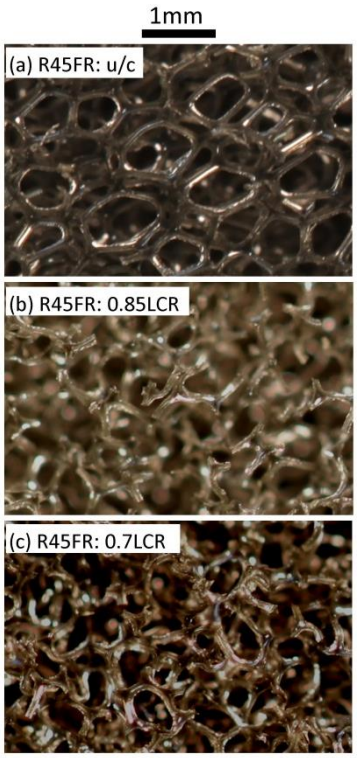

Figure 3 Through thickness images of cell structure obtained for the R45FR foams.

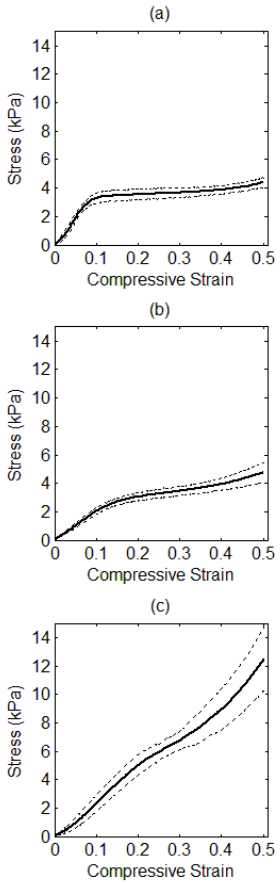

Figure 4 Mean quasi-static compressive stress-strain plots averaged across the three foam types, a) unconverted, b) 0.85 LCR and c) 0.7 LCR. The dotted lines represent one standard deviation either side.

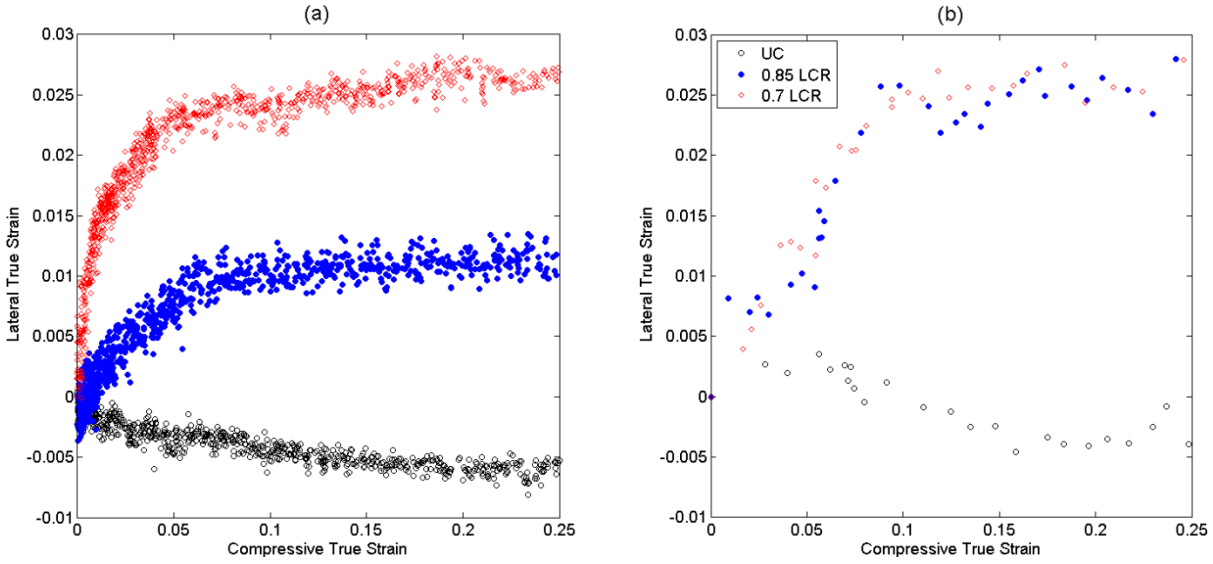

Figure 5 Sample lateral strain vs longitudinal strain plots for R60 foam, a) quasi-static, Poisson's ratio at 10% true strain was -0.03 for 0.7 LCR, 0.13 for 0.85 LCR and 0.21 for UC and b) 4 J impacts, Poisson's ratio at 10% true strain was -0.04 for 0.7 LCR, 0.24 for 0.85 LCR and 0.25 for UC.

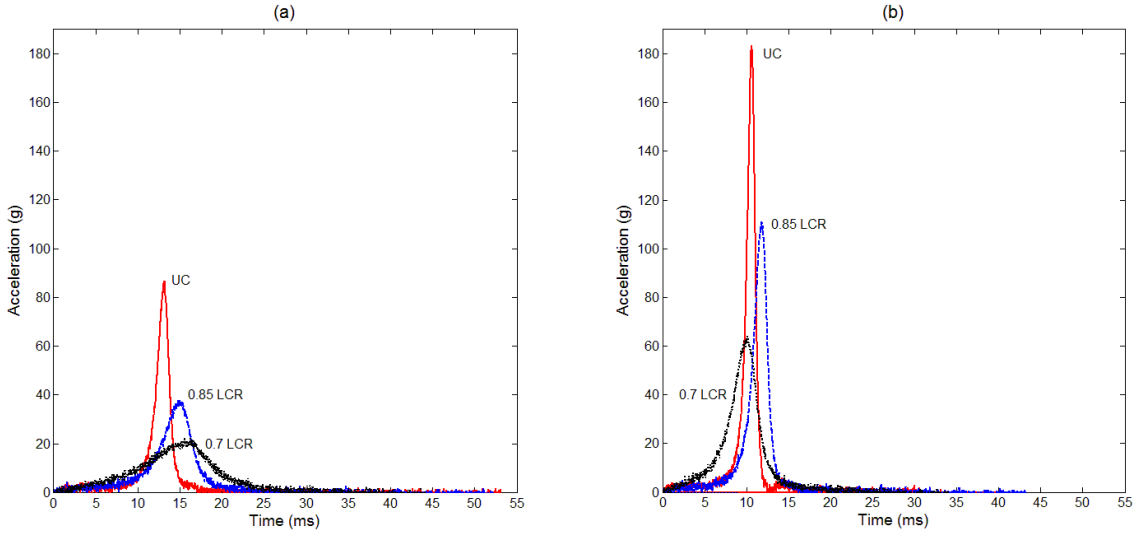

Figure 6 Sample accelerometer traces for the flat dropper on the R45 foam, a) 2 J and b) 4 J. Peak acceleration was synchronised with maximum deformation from video footage and the start and end of the contact was identified from the video.

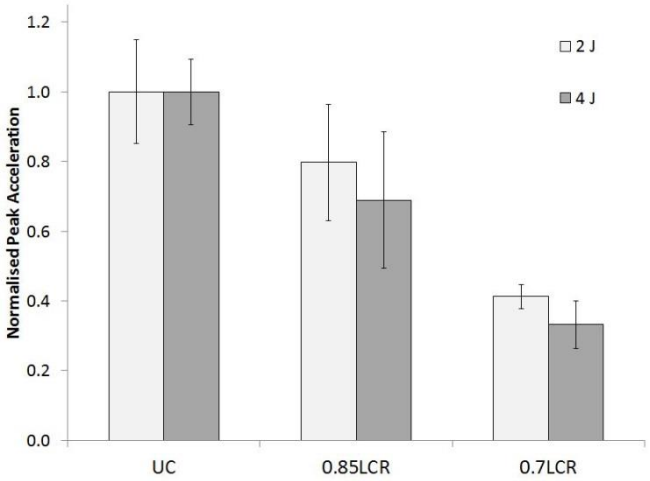

Figure 7 Flat dropper normalised peak acceleration mean for all 3 foams. 2 J impacts normalised to UC mean of 64 g, 4 J impacts normalised to UC mean of 182 g. Error bars correspond to one SD either side.

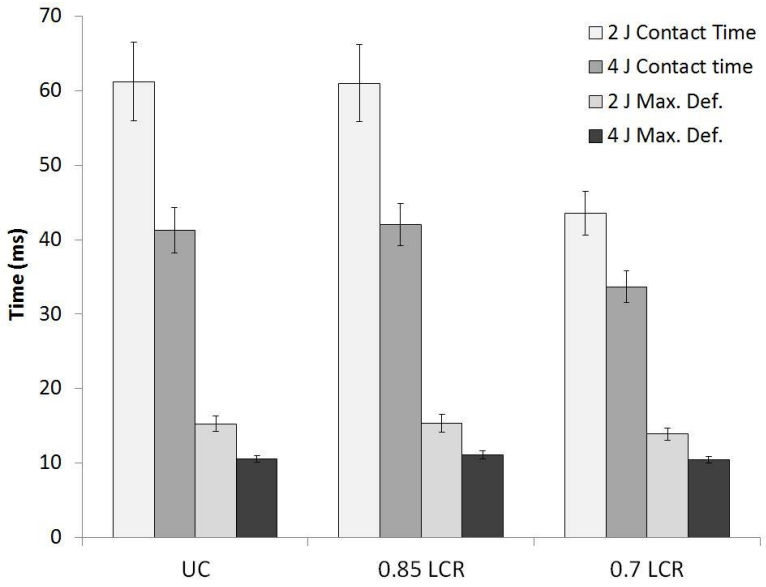

Figure 8 Flat faced dropper contact time and time to maximum deformation averaged across the three foam types. Error bars correspond to one SD either side.

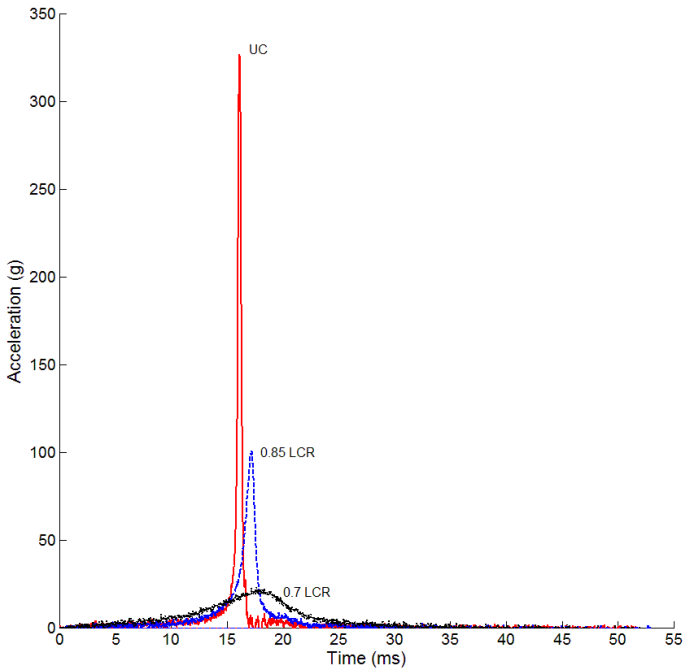

Figure 9 Sample accelerometer traces for the hemispherical dropper on the R45 foam. Peak acceleration was synchronised with maximum deformation from video footage and the start and end of the contact was identified from the video.

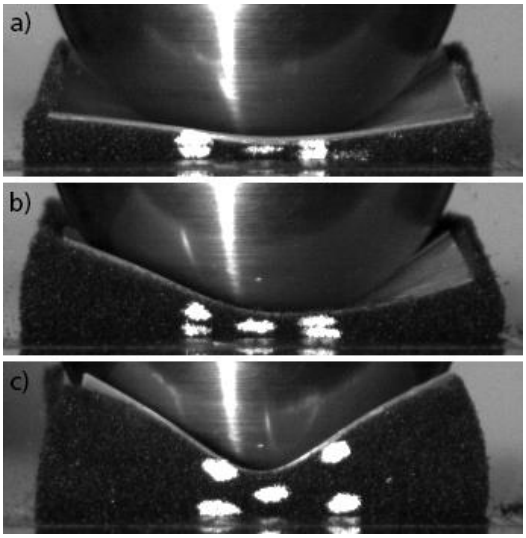

Figure 10 Maximum deformation of the hemispherical dropper on the R45 foam, a) unconverted at 16 ms, b) 0.85 LCR at 17 ms and c) 0.7 LCR at 18 ms.

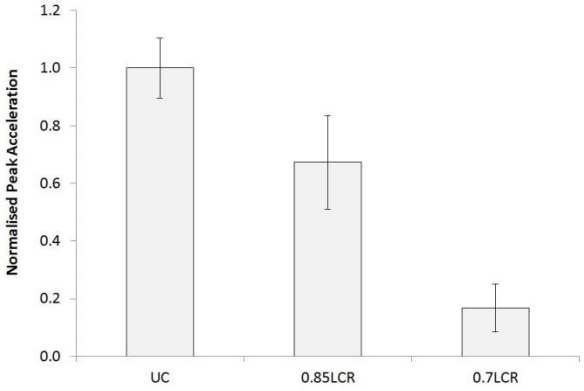

Figure 11 Hemispherical dropper normalised peak acceleration for 2 J impacts. Normalised to UC mean of 327 g. Error bars correspond to one SD either side.